High-resolution angle-resolved photoemission study of LaSb

H. Kumigashira, Hyeong-Do Kim, T. Ito, A. Ashihara, T. Takahashi, T. Suzuki, M. Nishimura, and O. Sakai
Department of Physics, Tohoku University, Sendai 980-8578, Japan

Y. Kaneta
Department of Quantum Engineering and Systems Science, Faculty of Engineering, The University of Tokyo, Tokyo 113-8586, Japan

H. Harima
The Institute of Scientific and Industrial Research, Osaka University, Ibaraki, Osaka 567-0047, Japan
(Received 30 March 1998; revised manuscript received 11 May 1998)

High-resolution angle-resolved photoemission spectroscopy (HR-ARPES) has been performed to study the electronic band structure of LaSb, which has no f electrons and is regarded as a nonmagnetic reference of CeSb and USb. HR-ARPES measurements near the Fermi level have established the existence of hole and electron pockets at the Brillouin-zone center and boundary, respectively, showing directly the semimetallic nature of LaSb. This supports the essential framework of the p-f mixing model to explain the anomalous magnetic properties of CeSb based on the semimetallic band structure of the mother compound. ARPES spectra of LaSb have been calculated based on the linear-muffin-tin-orbital band structure to interpret the experimental result. The ''band structure'' obtained by ARPES is contributed to considerably by stationary lines with the zero group velocity ($v_g = \partial E/\partial k = 0$) midway between high-symmetry lines in the Brillouin zone. The overall feature of the band structure shows an excellent agreement between the experiment and the calculation while the Sb $5p_{3/2}$ bands that give two holelike Fermi surfaces at the Γ point are situated at higher binding energy by 0.3 eV in the calculation than in the experiment. Possible origins for the observed discrepancy are discussed. [S0163-1829(98)05736-1]

I. INTRODUCTION

The electronic structure of LaSb, in particular its Fermi surface (FS) topology, has been intensively studied theoretically[1,2] and experimentally,[3–5] because LaSb has no $4f$ electrons and is regarded as a good nonmagnetic reference to CeSb and USb, which exhibit anomalous physical properties originating in the highly correlated f electrons.[6–10] The observed anomalous magnetic and electronic properties of Ce monopnictides (CeXp; Xp=N–Bi) are well explained by the p-f mixing model,[11] which is based on the semimetallic band structure of the mother compound LaXp and the strong anisotropic hybridization between the pnictogen $np_{3/2}$ ($n=2-6$) state and the crystal-field-split level of the Ce $4f$ state. We have already performed high-resolution angle-resolved photoemission spectroscopy (HR-ARPES) measurements on some Ce monopnictides[12–15] and found a systematic change of the FS topology across the magnetic phase transition in CeSb (Refs. 14 and 15) as predicted by the p-f mixing model. This supports the essential framework of the p-f mixing model. However, there remain some unresolved problems in the electronic structure. For example, we observed a pseudogaplike structure around 2 eV binding energy in the electronic structure of CeSb.[14,15] It is not clear whether this gaplike structure is related to the existence of occupied $4f$ states. We performed the ARPES measurements at two different temperatures over the magnetic phase transition of CeSb and found the change of the FS topology, as described above, but at the same time we found that the overall dispersion of bands for the magnetically ordered phase with a tetragonal unit cell is essentially the same as that of the paramagnetic phase with fcc crystal structure.[14,15] The effect of symmetry lowering caused by the magnetic order such as band folding was not clearly seen in the ARPES experiment. In order to obtain insight into these unresolved problems as well as to understand the anomalous properties of CeSb based on the p-f mixing model, the detailed band structure of the mother compound LaSb is necessary.

In this paper, we report results of HR-ARPES on LaSb, together with the band-structure calculation using the linear-muffin-tin-orbital (LMTO) method. We calculated theoretical ARPES spectra to interpret the experimental results and found that the experimental ''band structure'' obtained by ARPES is contributed to considerably by stationary lines with zero-group velocity ($v_g = \partial E/\partial k = 0$) midway between high-symmetry lines in the Brillouin zone (BZ) as well as by the high-symmetry lines with high density of states. In HR-ARPES measurements, we clearly observed hole and electron pockets at the BZ center and boundary, respectively, indicative of the semimetallic nature of LaSb. While we found an excellent agreement in the overall feature of the valence-band structure between the HR-ARPES result and the band-structure calculation, we also observed some quantitative discrepancies. We discuss the electronic band structure of LaSb by comparing the present HR-ARPES result with the band-structure calculation as well as the reported de Haas–van Alphen (dHvA) results.[3–5]

II. EXPERIMENT

LaSb single crystals were grown by the Bridgman method with a sealed tungsten crucible and a high-frequency induction furnace. High-purity La ($3N$) and Sb ($5N$) metals with

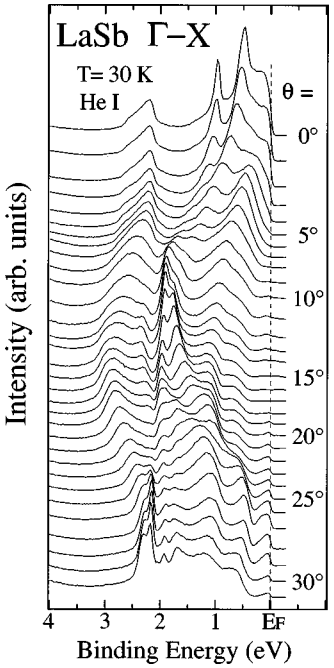

FIG. 1. High-resolution angle-resolved photoemission spectra of LaSb measured for the ΓXXX plane in the Brillouin zone with the He I resonance line (21.22 eV) at 30 K. The polar angle (θ) referred to the surface normal is indicated.

the respective composition ratio were used as starting materials. The obtained samples were characterized by the Debye-Scherrer method as well as the resistivity and transversal magnetic resistance measurements. The obtained lattice constant, residual resistivity at 4.2 K, and magnetoresistivity $[\Delta\rho/\rho(0)$ where $\Delta\rho=\rho(10\,T)-\rho(0)]$ at 0.8 K were 6.499 Å, 0.5 $\mu\Omega$ cm, and 150, respectively. These values are almost the same as those of a single crystal with which the dHvA signal was observed.[3–5]

Photoemission measurements were carried out using a homebuilt high-resolution angle-resolved photoemission spectrometer, which has a large hemispherical electron energy analyzer (diameter: 300 mm) and a very bright discharge lamp. The base pressure of the spectrometer is 2×10^{-11} Torr and the angular resolution is about $\pm1°$. The energy resolution was set at 50 meV for quick data acquisition because of relatively fast degradation of the sample surface. A clean mirrorlike surface of the LaSb (001) plane was obtained by *in situ* cleaving at 30 K just before the measurement and kept at the same temperature during the measurement. Since we observed degradation of the sample surface as evident by increase of background in the spectrum, we recorded all spectra before the spectral change became detectable. The Fermi level (E_F) of the sample was referred to that of a gold film evaporated onto the sample substrate and its accuracy is estimated to be better than 5 meV. We performed photoemission measurements on several samples and confirmed that the results are reproducible.

III. RESULTS

A. Angle-resolved photoemission spectra

Figure 1 shows the HR-ARPES spectra of LaSb measured at $T=30$ K along the [010] direction in the fcc Brillouin zone (see Fig. 2). The polar angle (θ) referred to the surface normal of the cleaved (001) plane is denoted. We find in Fig. 1 that HR-ARPES spectra exhibit remarkable and systematic changes as a function of polar angle. In the near-E_F region, we find a broad band dispersing toward the high binding energy from $\theta=0°$ to about 15° as well as a small structure just at E_F around the BZ boundary ($\theta=20°-30°$).

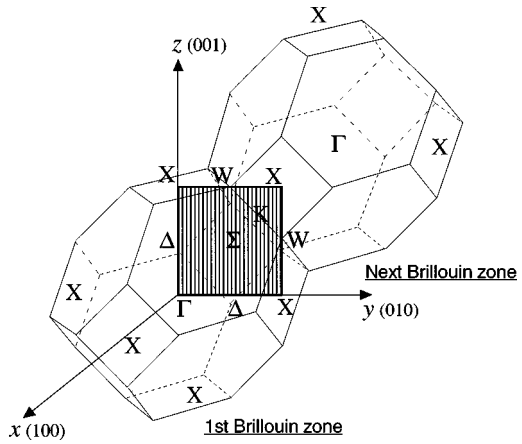

FIG. 2. The Brillouin zone of LaSb in the extended zone scheme (thin lines). HR-ARPES measurement was performed for the ΓXXX plane. The 1D DOS along $k_\perp$ (parallel to the z axis) was calculated at different 101 $k_\parallel$ (parallel to the y axis) points in the ΓXXX plane to interpret the experimental result.

In order to see the spectral changes near E_F in detail, we show in Fig. 3 the spectra near E_F in an enlarged binding-energy scale. We find in Fig. 3 that there are at least three

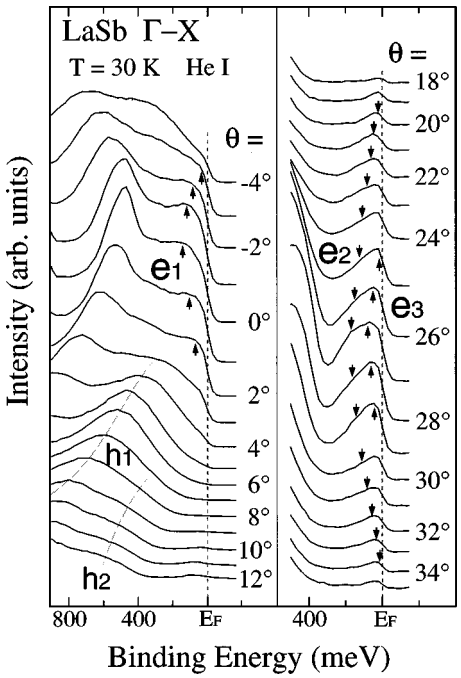

FIG. 3. High-resolution angle-resolved photoemission spectra near E_F of LaSb measured for the ΓXXX plane with the He I line at 30 K. The polar angle referred to the surface normal is indicated on each spectrum. Guides (arrows and thin broken lines) are shown for the eyes to indicate possible energy dispersion.

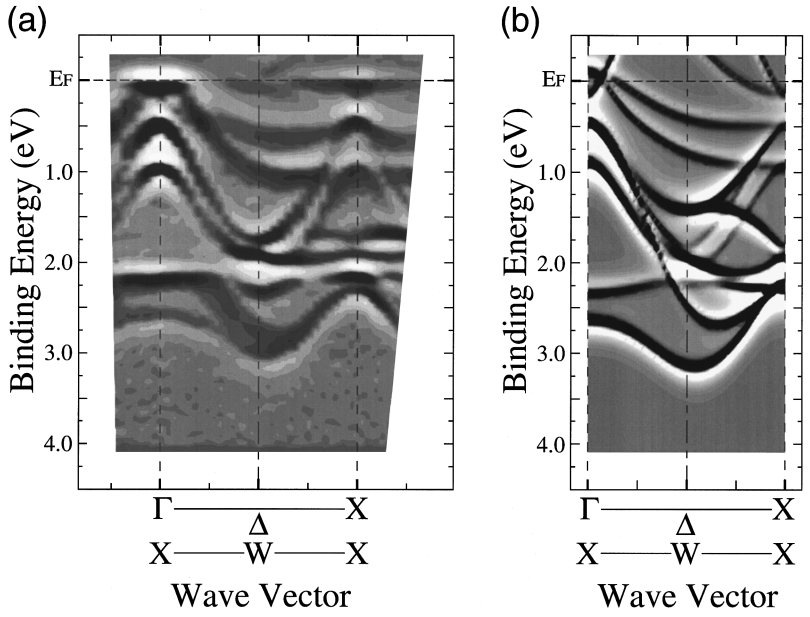

FIG. 4. (a) Experimental band structure of the ΓXXX plane of LaSb determined by the present HR-ARPES measurement. Dark parts correspond to the energy bands. (b) Theoretical ARPES-derived band structure of LaSb obtained by the LMTO band-structure calculation. For details, see text.

bands (h_1, h_2, and e_1), which seem to cross E_F around $\theta=0°$. Bands h_1 and h_2 appear to have a similar energy dispersion. The band h_1 gradually approaches E_F with decreasing θ from about 10° and crosses E_F somewhere in the range of $\theta=0°-2°$, while it is difficult to identify the E_F-crossing point of the h_2 band due to the low intensity as well as its close proximity of the stronger h_1 band. Since these two bands (h_1 and h_2) have their major part in the occupied states below E_F, they give holelike Fermi surfaces. We find another band e_1 around $\theta=0°$ that gives an electronlike FS. The band e_1 suddenly appears at E_F at $\theta=2°$, where the band h_1 accidentally crosses E_F from the occupied states. The appearance of the additional band e_1 in the occupied states is evident from the increase of intensity and the shift of the near-E_F peak from $\theta=2°$ to 0°. Since this near-E_F band enters again the unoccupied states around $\theta=-2°$, this band gives an electronlike FS. All these results suggest the existence of two hole pockets and one electron pocket around Γ and/or X point in the BZ (see Fig. 2) since $\theta=0°$ corresponds to the line along ΓX direction.

On the other hand, in the region of larger polar angles of $\theta=18°-34°$ we observe at least two bands near E_F. On increasing the polar angle from 18°, one band (e_2) suddenly appears at E_F at $\theta=19°-20°$, showing a small energy dispersion with the maximum binding energy of about 200 meV at $\theta=27°$, approaching again toward E_F, and finally enters the unoccupied states around $\theta=34°$. We find another band (e_3) appearing at E_F at $\theta=24°-25°$. The existence of the band e_3 is confirmed by the sudden increase of the spectral intensity at E_F at $\theta=25°$ as well as the two-peak structure observed in the spectrum at $\theta=27°$. These two bands give electron pockets around X point since the polar angle ($\theta=27°$) approximately corresponds to the XX line (see Fig. 2). It is noticed here that the dispersive feature of band e_3 looks very similar to that of band e_1 observed in the ΓX line, suggesting the same origin for both bands.

Figure 4(a) shows the experimental ''band structure'' of LaSb derived from the present HR-ARPES measurement. In order to map out the ''band structure,'' we took the second derivative of ARPES spectra after moderate smoothing and plotted the intensity in a square-root scale by gradual shading as a function of the wave vector and the binding energy;[16] dark parts correspond to ''bands.'' We set the gray-scale image in Fig. 4(a) so as to have the apparent bandwidth in the gray-scale image being almost equal to the full width at half-maximum of the corresponding band in Figs. 1 and 3. We used the smoothing in order to delete spiky noises in the spectra and confirmed that the essential spectral shape is unchanged through this procedure. As found in Fig. 4(a), the obtained energy bands are symmetric with respect to Γ and X points in the BZ, indicating their characters being of bulk origin.

B. Analysis of ARPES spectra

It is well known that an ARPES spectrum of a three-dimensional material is classified into two cases, the ''bulk'' and ''band-gap'' cases.[17] The momentum perpendicular to the surface ($k_\perp$) dose not conserve in the band-gap case because of lack of appropriate final states in the photoexcitation process, while it conserves in the bulk case. The present ARPES measurement of LaSb with He I (21.22 eV) photons seems to belong to the band-gap case, because (1) we observe at least eight bands in the ΓXXX plane while the band-structure calculation[1,2] predicts only four bands in the same plane in the energy range of 0–5 eV binding energy and (2) the observed energy bands are symmetric with respect to the $X(X)$ point at the BZ boundary, which is not expected in the bulk case because of conservation of $k_\perp$.[16] It is well established that high-symmetry lines in the BZ with zero group velocity ($v_g=\partial E/\partial k=0$) are likely to appear as prominent well-resolved structures in the ARPES spectrum of the

band-gap case, because the density of states is relatively larger on the high-symmetry lines.[18] It is also expected that a stationary point (line) midway between the high-symmetry lines may appear as a strong structure in the ARPES spectrum since the group velocity is also zero on the point (line).

In order to analyze the experimental band structure, we performed the band-structure calculation for the ΓXXX plane and calculated the one-dimensional density of states (1D DOS) along $k_\perp$. We employed the LMTO method with the potential obtained from the linear augmented plane-wave (LAPW) method with local-density approximation (LDA).[2] Since we found that the overlapping between the conduction band and the valence band is too large in the self-consistent calculation, we introduced an empirical level correction (ELC) for the La $5d$ level.[19] Next, in order to mimic the ARPES spectrum from the ΓXXX plane, we calculated the 1D DOS along $k_\perp$ as follows. Firstly, we defined a square mesh on the ΓXXX plane with 101 $k_\parallel$'s and 16 $k_\perp$'s and calculated the band energy at each ($1616=101\times16$) point. Then, using the spline interpolation method, we obtained the band dispersions along $k_\perp$ at each $k_\parallel$. We determined the group velocity (v_g) by taking the derivative of the band dispersion and created the 1D DOS at each $k_\parallel$ by integrating the $1/v_g$ along $k_\perp$. Thus, we obtained 101 theoretical ARPES spectra by convoluting the 1D DOS with a Lorentzian with a 50 meV width. Finally by applying the same procedure (but without smoothing) to these theoretical ARPES spectra, we mapped out the theoretical ARPES-derived band structure for the ΓXXX plane as shown in Fig. 4(b). It is noted here that besides the two high-symmetry lines (Γ-X and X-W-X) some stationary lines (points) midway between the two high-symmetry lines appear as ''dispersive bands'' in the theoretical ARPES-derived band structure. In order to identify the origin of bands, we show in Fig. 5 the calculated band dispersions with different symbols. White solid and dashed lines correspond to the bands along Γ-X and X-W-X high-symmetry lines, respectively, while triangles, crosses, and quadrilaterals show the stationary lines with $v_g=0$ between the two high-symmetry lines. The trajectory of the stationary lines in the ΓXXX plane is shown with the same symbols in the lower panel of Fig. 5. We also label the calculated bands, $a-k$ for further clarification. In Fig. 5, the calculated band structure is superimposed with the experimental band dispersion derived from ARPES for comparison.

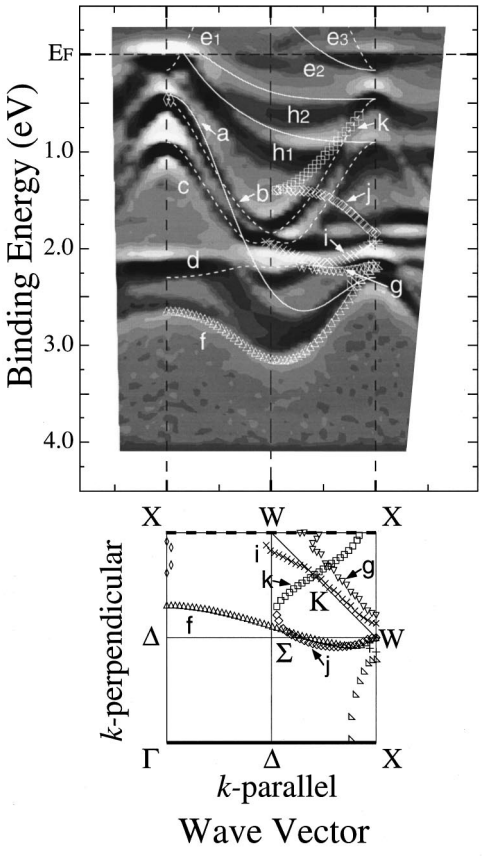

FIG. 5. Experimental band structure of LaSb derived by HR-ARPES experiment (gray scale) compared with the stationary lines with v_g (group velocity)$=0$ in the band-structure calculation (solid and broken lines, and white symbols). Each calculated band is labeled ($a-k$). Trajectories of the stationary lines (points) in the ΓXXX plane are shown in the lower panel with the same symbols.

IV. DISCUSSION

According to the band-structure calculation,[1,2] the top of the occupied electronic states of LaSb consists mainly of the Sb $5p$ states, which split into the $5p_{3/2}$ (Γ_8) and $5p_{1/2}$ (Γ_6) bands by the spin-orbit interaction, while the bottom of the unoccupied states originates in the La $5dt_{2g}$ states. The calculation predicts that LaSb should be semimetallic due to the overlap of the Sb $5p_{3/2}$ and La $5dt_{2g}$ bands, which produces two hole pockets with a dominant Sb $5p_{3/2}$ character at the Γ point and an electron pocket with the La $5d$ nature at the X point.[1,2] As found in Figs. 4 and 5, the experimental result is in good agreement with the band-structure calculation. In particular, bands b and c originating in the X-W-X high-symmetry line (dashed line) show an almost perfect agreement in the energy range of 0.3–2.0 eV. On the other hand, on the Γ-X high-symmetry line (solid line), bands h_1 and h_2, which form hole pockets around the Γ point, are located at slightly higher binding energies in the experiment than in the calculation.

When we look at the higher binding-energy region, we find that there are at least three dispersive bands at 2–3 eV in the experiment; one is the lowest band, which has the bottom of the dispersion at 3 eV, the next one is the second-lowest band, which has a dispersion similar to that of the former one in the right half of the ΓXXX plane but is located at the smaller binding energy in the left half of the plane, and the third experimental band is located around 2.2 eV and is almost dispersionless. When we compare the experimental band dispersions with the calculation, the lowest experimental band is assigned to the calculated band *f*, which originates in the stationary line with $v_g=0$ between the two high-symmetry lines. We find that the band f is situated at a slightly higher binding energy in the calculation than in the experiment. The third experimental band may be ascribed to the almost flat band calculated along the X-W-X line (band d in the calculation), although the curvature of the band around the W point looks different in the experiment than it does in the calculation.

The second experimental band located between bands d and f appears not to have a counterpart in the calculation. We

assign this experimental dispersive band to a part of the highly dispersive Sb $5p_{1/2}$ band (band *a* in the calculation). We find that the band *a* is located at 0.5 and 2.3 eV at the Γ and *X* points, respectively, and shows the bottom at 2.6 eV midway between the Γ and *X* points. The reason for this assignment is following. Since the normal emission spectrum ($\theta=0°$) corresponds to the 1D DOS along the Γ-*X* high-symmetry line, the bottom of the experimental band *a* in the Γ-*X* high-symmetry line should be located at 2.6 eV as shown in Figs. 4(a) and 5. Further, as described above, comparison of the experiment and the calculation shows that the bottom of band *a* is not on the high-symmetry line but is situated midway between. This means that when we trace the band *a* by changing the polar angle along the Γ-*X* line, the band should have a stationary (minimum) point between Γ and *X* point. We find that this is the case in the calculation, since the band *a* has a minimum point at 2.6 eV midway between Γ and *X* points and this energy coincides with the energy of band *f* at Γ point which corresponds to the bottom of the Sb $5p_{1/2}$ 1D DOS calculated for the normal-emission spectrum ($\theta=0°$). Thus, the broad dispersive band located at 2.2–3 eV is assigned to a part of the highly dispersive band *a*. The observed broadness may be due to a small v_g of the band (in other words, flat feature of the band) in this energy and momentum region. As found in Figs. 4(a) and 5, we could not well resolve this Sb $5p_{1/2}$ band (band *a*) in the binding-energy region of 0.5–2.2 eV in the experiment. This may be due to the highly dispersive feature of the band since in general a band with a large v_g gives a small and weak structure in the ARPES spectrum owing to the finite angular resolution. Further, strong photoemission peaks coming from the *X*-*W*-*X* line may cover this highly dispersive Sb $5p_{1/2}$ band since they are very close to each other in the left half of the ΓXXX plane as found in Fig. 5. Thus, we infer that the pseudo-gap-like structure observed at 2 eV may not be intrinsic but is produced by accidental overlapping and/or crossing of several bands in this energy and momentum region. This also suggests that a similar pseudogaplike structure observed in CeSb (Refs. 14 and 15) is not related to the existence of occupied $4f$ states.

In Figs. 4(a) and 5, we find two flat experimental bands at 1.8 and 2 eV, respectively, in the right half of the ΓXXX plane. These two dispersionless bands may be assigned to calculated bands *j* and *i*, respectively, which originate in the stationary lines with $v_g=0$ of bands *b* and *c*, respectively. This indicates that band *j* has a much larger energy dispersion in the calculation than in the experiment, while the other one (band *i*) shows relatively good agreement. The discrepancy in the energy of band *j* may be due to underestimation of the hybridization strength between the Sb $5p$ and the La $5d$ states around the center of the ΓXXX plane, since the stronger hybridization would cause a downward shift of the Sb $5p$ band.

The FS topology of LaSb was already studied by dHvA measurements.[3–5] The observed FS consists of three different sheets; a small and a large hole FS: (named β and γ sheets, respectively[3]) at Γ point and an electron FS (α sheet) at the *X* point. When we compare the present ARPES results with the dHvA measurements, we immediately notice that h_1 and h_2 bands in Fig. 3 should correspond to the bands that form the small and the large hole sheets, respectively. However, as seen in Figs. 4 and 5, the E_F-crossing point of both experimental h_1 and h_2 bands looks almost the same while the corresponding calculated bands intercept E_F at different points. The experimental E_F-crossing point appears to coincide with that of the calculated h_1 band, which gives a small holelike FS sheet. It is noted here again that the calculation underestimates the binding energy of both h_1 and h_2 bands by about 0.3 eV midway between Γ and *X* points as seen in Figs. 4 and 5. When we pull down the calculated h_2 band to fit the experimental h_2 band, the E_F-crossing point would move toward the Γ point, thereby giving better agreement with the experiment. However, in light of the fact that the present band-structure calculation gives the FS volume consistent with the dHvA measurement, the experimental h_2 band should intercept E_F far away from the Γ point compared with the calculation in other directions of the BZ. This point should be examined in future ARPES experiments.

Next, we discuss the electron pocket. The band-structure calculation[1,2] has predicted that an electron pocket is located at the *X* point, forming an ellipsoidal FS with the longer axis in the Γ-*X* direction. The dHvA measurements[3–5] have assigned one of the observed branches (α sheet) to this electron pocket. In ARPES measurements, on the other hand, we observed three electron pockets in the ΓXXX plane, as seen in Fig. 4. The appearance of three electron pockets in the present ARPES measurement is understood as follows. In the present study, we performed ARPES measurements for the (001) cleaved plane by changing the polar angle from the [001] direction to the [010] direction. Under this experimental setup, we observe the electronic structure of the whole ΓXXX plane in the BZ as described above. Therefore, when we start the ARPES measurement from $\theta=0°$, we at first observe a small electron pocket at the *X* point located on the *z* axis in Fig. 2 (which corresponds to band e_1 in Fig. 3). Since the ellipsoidal FS has the longer axis in the Γ-*X* direction, we cross the FS along the shorter axis. On further increasing the polar angle, we then reach the second (but equivalent to the first one) electron pocket located at the *X* point on the *y* axis, which corresponds to band e_2 in Fig. 3. Since the FS is elongated in the Γ-*X* direction, we touch the electronlike FS from the longest axis. Shortly after passing the second FS, we finally reach the third one located on the *X* point on the diagonal line with respect to Γ point in the ΓXXX plane (see Fig. 2). Because of the same reason described above, we cross the FS along the shorter axis. The third FS corresponds to band e_3 in Fig. 3. Thus, we observe three electron pockets which should be identical to each other but have different orientations by 90°. This, in turn, enables us to measure directly the size of each axis of the ellipsoidal electron FS as well as the exact location in the BZ. It is noted here that the present ARPES observation is in good agreement with the band-structure calculation as well as with the dHvA result[3–5] as seen in Fig. 5.

Next, we compare the experimental band structure of LaSb derived by HR-ARPES with that of CeSb which undergoes a series of magnetic phase transitions with temperature from paramagnetic phase at high temperature to antiferromagnetic phase at low temperature.[14,15] We observed a small but distinct change in the FS topology (volume) across the magnetic phase transition in CeSb, but did not clearly see an effect of symmetry lowering caused by the magnetic order

such as band folding. We find that the overall structure of experimental band dispersion is essentially the same among LaSb, paramagnetic and antiferroparamagnetic CeSb.[14,15] This implies that the symmetry lowering caused by the magnetic order may have a very small effect on the electronic structure observed by the ARPES experiment.

Finally, we discuss the quantitative discrepancy between the experiment and the band calculation, in particular, in the energy dispersion of Sb $5p_{3/2}$ bands (h_1 and h_2 bands in Fig. 5). As seen in Fig. 5, these two Sb $5p_{3/2}$ bands that give holelike FS's at the Γ point are situated closer to E_F in the calculation than in the experiment. This discrepancy is crucial for quantitative understanding of the anomalous magnetic properties of CeSb based on the p-f mixing model. Two possible origins are inferred to account for this discrepancy. One is underestimation of the hybridization strength between the Sb $5p_{3/2}$ and the La $5d$ states in the calculation, since the hybridization matrix is stronger midway between Γ and X points; actually it is zero at Γ and X points. Another possible origin for the discrepancy is underestimation of the hybridization strength between the Sb $5p_{3/2}$ and the unoccupied La $4f$ state, which is the strongest at Γ point. In order to check these two possibilities, we have performed several band-structure calculations with different empirical level correction (ELC) terms for the La $5d$ level.[19] The result shows that the dispersion of conduction bands is very sensitive to the ELC parameter while that of Sb $5p_{3/2}$ bands on the Γ-X line is not. This suggests that the observed discrepancy in the energy position of the Sb $5p_{3/2}$ bands may be due to underestimation of the hybridization between the Sb $5p_{3/2}$ and the unoccupied La $4f$ state. However, a simple increase of the hybridization strength in the present calculation causes an downward shift of the Sb $5p_{3/2}$ bands near the Γ point, resulting in decrease of the FS volume. This causes discrepancy to the dHvA result[3–5] since the present band calculation gives the FS volume consistent with the dHvA measurement. Thus, a more elaborate band-structure calculation with reasonable parameters is necessary to understand both the dHvA and the ARPES experimental results.

V. CONCLUSION

We have performed high-resolution angle-resolved photoemission spectroscopy (HR-ARPES) on single crystal LaSb to study the band structure and the Fermi-surface topology. HR-ARPES measurements near the Fermi level have established the existence of hole and electron pockets at the Brillouin-zone center and boundary, respectively, indicative of the semimetallic nature of LaSb. We have performed the LMTO band structure calculation to interpret the HR-ARPES results and found that the overall feature of the valence-band structure shows a good agreement between the HR-ARPES experiment and the calculation while there is a quantitative discrepancy in the energy position of the Sb $5p_{3/2}$ bands. The present HR-ARPES observation of holelike and electronlike Fermi surfaces in LaSb supports the p-f mixing model which explains the anomalous magnetic properties of CeSb based on the semimetallic band structure of the mother compound LaSb. The observed quantitative discrepancy requests a more elaborate band structure calculation.

ACKNOWLEDGMENTS

The authors are grateful to Professor A. Hasegawa at Niigata University for useful discussion. H.K. thanks the Japan Society for the Promotion of Science for financial support. This work was supported by grants from the REIMEI Research Resources of Japan Atomic Energy Research Institute and the Ministry of Education, Science, and Culture of Japan.

[1] A. Hasegawa, J. Phys. Soc. Jpn. **54**, 677 (1985).
[2] Y. Kaneta, O. Sakai, and T. Kasuya, Physica B **186–188**, 156 (1993).
[3] H. Kitazawa, T. Suzuki, M. Sera, I. Oguro, A. Yanase, A. Hasegawa, and T. Kasuya, J. Magn. Magn. Mater. **31–34**, 421 (1983).
[4] R. Settai, T. Goto, S. Sakatsume, Y. S. Kwon, T. Suzuki, and T. Kasuya, Physica B **186–188**, 176 (1993).
[5] N. Môri, Y. Okayama, H. Takahashi, Y. Haga, and T. Suzuki, Jpn. J. Appl. Phys., Suppl. **8**, 182 (1993).
[6] R. Settai, T. Goto, S. Sakatsume, Y. S. Kwon, T. Suzuki, Y. Kaneta, and O. Sakai, J. Phys. Soc. Jpn. **63**, 3026 (1993).
[7] M. Takashita, H. Aoki, T. Matumoto, C. J. Haworth, T. Terashima, A. Uesawa, and T. Suzuki, Phys. Rev. Lett. **78**, 1948 (1997).
[8] J. Schoenes, B. Frick, and O. Vogt, Phys. Rev. B **30**, 6578 (1984).
[9] H. Rudigier, H. R. Ott, and O. Vogt, Phys. Rev. B **32**, 4584 (1985).
[10] Q. G. Sheng, B. R. Cooper, and S. P. Lim, Phys. Rev. B **50**, 9215 (1985).
[11] H. Takahashi and T. Kasuya, J. Phys. C **18**, 2697 (1985).
[12] H. Kumigashira, S.-H. Yang, T. Yokoya, A. Chainani, T. Takahashi, A. Uesawa, T. Suzuki, O. Sakai, and Y. Kaneta, Phys. Rev. B **54**, 9341 (1996).
[13] H. Kumigashira, S.-H. Yang, T. Yokoya, A. Chainani, T. Takahashi, A. Uesawa, and T. Suzuki, Phys. Rev. B **55**, R3355 (1997).
[14] H. Kumigashira, H.-D. Kim, A. Ashihara, A. Chainani, T. Takahashi, A. Uesawa, and T. Suzuki, Phys. Rev. B **56**, 13 654 (1997).
[15] T. Takahashi, H. Kumigashira, T. Ito, A. Ashihara, H.-D. Kim, H. Aoki, A. Ochiai, and T. Suzuki, J. Electron Spectr. Relat. Phenom. **92**, 65 (1998).
[16] F. J. Himpsel, Adv. Phys. **32**, 1 (1983).
[17] P. J. Feibelman and D. E. Eastman, Phys. Rev. B **10**, 4932 (1974).
[18] T. Grandke, L. Ley, and M. Cardona, Phys. Rev. B **18**, 3847 (1978).
[19] In general, LDA band calculation is likely to overestimate the overlapping between conduction and valence bands. In order to compensate for this overestimation, the ELC for the orbital that forms the conduction bands has been introduced so as to reproduce the dHvA data. In the present LMTO calculation, we added an extra pseudopotential expressed as $H_p=\Sigma_{lm}|\phi_{lm}>\Delta\varepsilon_l<\phi_{lm}|$ in the muffin-tin sphere (MTS), where ϕ_{lm} denotes the atomiclike orbit that has the $r^{-(l+1)}$ tail in the outer region of the MTS. We have raised the La $5d$ level by $\Delta\varepsilon_{5d}=1.12$ eV to compensate the overlapping between the Sb $5p$ and the La $5d$ band.